Quasi-static Finite Element Analysis of C2–T1 Spine Kinematics with Inclusion of T2 Vertebra: Relevance to Cervical Spine Biomechanics

Febin Chris Asir J A, Balaji Harinathan, Davidson Jebaseelan D, Pugazhenthi Subramanian Kalaimani, Karthik Banurekha Devaraj, Aju Bosco, Aditya Vedantam and Narayan Yoganandan

Abstract Finite element (FE) models of the cervical spine commonly terminate at T1, which may introduce boundary condition artifacts that alter segment mechanics, particularly with studies that includes C7T1. This is relevant in multilevel surgical constructs that terminate at C7, leaving C7T1 as the inferior adjacent segment. This study evaluated whether incorporating the T2 vertebra into a validated C2–T1 FE model influences sagittal plane biomechanics and its boundary-related artifacts. A T1–T2 functional spinal unit (FSU) was developed and validated against post-mortem human subject (PMHS) data, then integrated into an existing C2–T1 model to create a C2–T2 model. Both models were subjected to 2 Nm flexion and extension moments in intact condition. Segmental range of motion (ROM) was compared between C2–T1 and the C2–T2 model, showed minimal differences in ROM (±4% in flexion, ±7% in extension) under a quasi-static loading. These results quantify the biomechanical effect of extending the model boundary from T1 to T2 under quasi-static loading. While the observed differences were minimal, they provide a baseline for future investigations for dynamic loads and for long fusion constructs.
Keywords Cervical spine, cervicothoracic junction, functional spine unit, finite element analysis, range of motion.

I. INTRODUCTION

The global demographic shift toward an aging population has led to a significant increase in osteoporosis prevalence, particularly among individuals over 60 years old [1]. This condition poses substantial challenges for spine surgeons, as osteoporotic bones often fail to provide stable fixation during single or bi-level spinal fusion procedures [2]. Consequently, there has been a growing trend toward performing longer fusion constructs, extending to levels such as C7 and/or T1, to enhance surgical stability and better accommodate the functional demands of elderly patients.

In cases involving multi-level fusions, particularly two, three, or four levels, the constructs often terminate at C7, leaving the C7T1 segment as an adjacent segment [3-5]. Finite element models (FEMs) and experimental studies have indicated that biomechanical alterations post-fusion can contribute to adjacent segment degeneration over time [3-4]. To accurately capture the changes, it is important to reduce the influence of boundary conditions in computational models. Current FEM studies commonly terminate at the T1 vertebra. For fusion procedures extending to C7, this approach may introduce boundary condition artifacts that may not reflect the biomechanical behaviour of the cervical spine. This study aims to address current models' limitation by incorporating the T2 vertebra into an existing C2–T1 finite element model [3-5] [13-14]. The current C2–T2 FEM, is used to evaluate how the addition of T2 vertebra affects overall spinal mechanics, and assess whether this approach reduces boundary condition artifacts.

II. METHODS

A detailed morphometric study of the thoracic vertebrae was carried out to identify the key parameters influencing their geometric structure (Fig 1). Geometrical data of the morphometric parameters, intervertebral disc (IVD) and ligaments were collected from existing literature [6-12] and normalised. Due to similarities in the geometrical features between the thoracic vertebra T2 and T1, the thoracic vertebra T1 was taken from a previously validated intact FEM of the cervical spine consisting of C2-T1 [13-14]. The C2–T1 finite element model, comprising all relevant components was validated for range of motion (ROM) across all motion planes by comparing its segmental ROM behavior [15] with experimental data reported from post-mortem human subject experiments [19]. Table1 details the material properties used for each component used in this study [16].

Febin Chris Asir J A is an undergrad engineering student and Davidson Jebaseelan is a Professor, Center for human movement analytics and school of mech.engg at Vellore Institute of Technology, Chennai, India (davidson.jd@vit.ac.in, +919445122485). Aju Bosco is a Professor and Spine Surgeon, Madras Medical College,Chennai,India Pugazhenthi Subramanian Kalaimani, Karthik Banurekha Devaraj, Balaji Harinathan are research associates and Aditya Vedantam is an Associate Professor and N. Yoganandan is a Professor at the Medical College of Wisconsin, Milwaukee, USA.

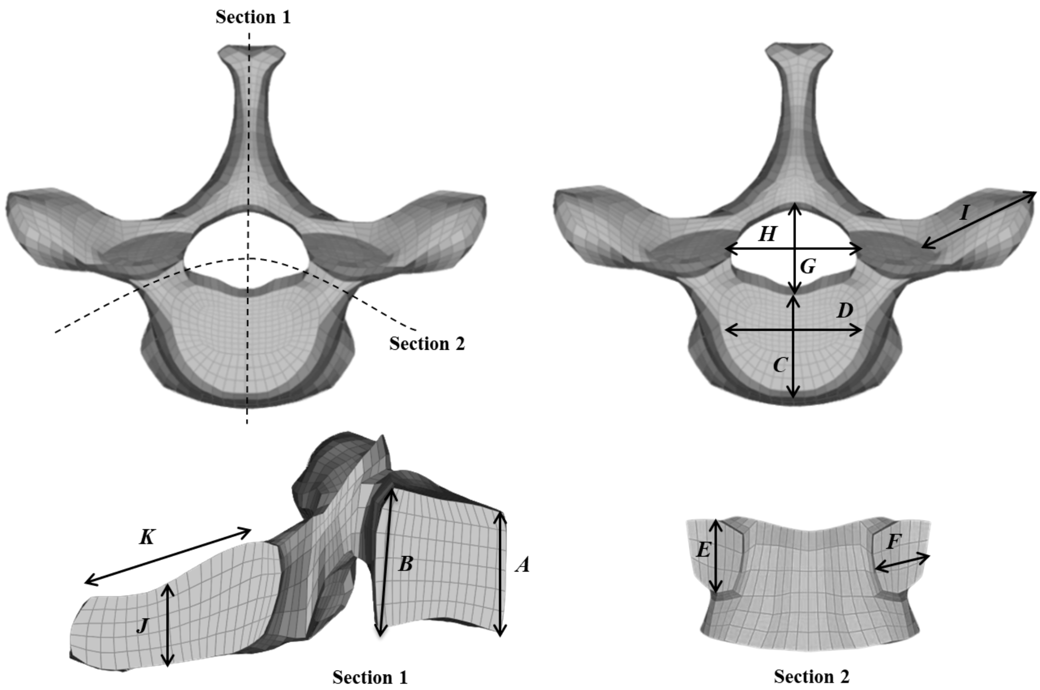

Fig. 1. Details the thoracic vertebra's morphometric parameters, where A represents Anterior Vertebral Body Height (AVBH), B is Posterior Vertebral Body Height (PVBH), C is Anterior-Posterior Diameter (APD), D is Transverse Diameter (TD), E is Pedicle Height (HP), F is Pedicle Width (WP), G is Spinal Canal Depth (SCD), H is Spinal Canal Width (SCW), I is Transverse Process Length (TPL), J is Spinous Process Length (SPL), and K is Spinous Process Height (SPH). Additional parameters, such as facet width and height included in this study, are not shown. The dimensions of the parameters are mentioned in table 2 and table 3 at the appendix section.

Table 1
Details the material properties used for each component in this study

Component	**Element type**	**Constitutive model**	**Parameters**
Cortical bone	Quadrilateral shell	Isotropic linear elastic	E = 16.8 GPa, μ = 0.3
Trabecular bone	Hexahedral solid	Isotropic linear elastic	E = 0.4 GPa, μ = 0.3
Endplate	Quadrilateral shell	Isotropic linear elastic	E = 5.6 GPa, μ = 0.3
Facet cartilage	Quadrilateral shell	Isotropic linear elastic	E = 0.01 GPa, μ = 0.3
Annulus ground substance	Hexahedral solid	Hill foam	n = 2, C1 = 0.000115 Gpa C2 = 0.002101 GPa, C3 = −0.000893 GPa b1 = 4, b2 = −1, b1 = −2
Annulus Fibers fibrosus	Quadrilateral shell membrane	Orthotropic nonlinear elastic	Fiber angle (45–60 deg)
Nucleus	Hexahedral solid	Fluid	K = 1720 MPa
Ligaments	Quadrilateral shell membrane	Nonlinear properties	Stress–strain curves
Intervertebral Cage	Tetrahedral Solid	Isotropic linear elastic	E = 110 GPa, μ = 0.3
Plate	Hexahedral solid	Isotropic linear elastic	E = 110 GPa, μ = 0.3
Screws	Tetrahedral Solid	Isotropic linear elastic	E = 110 GPa, μ = 0.3

Computational Modelling

Using a mapping- block based morphing technique [17], the FEM of T2 vertebra was developed. The functional spine unit (FSU) T1-T2 consisted of the vertebrae T1 and T2, which are connected by the IVD and a set of primary ligaments namely anterior longitudinal ligament (ALL), posterior longitudinal ligament (PLL), interspinous ligament (ISL), ligamentum flavum (LF), and capsular ligament (CL). The FEM was modelled using ANSA software (BETACAE Systems, MI, USA) and solved using LS-DYNA (R.11.0.0). The developed T1-T2 FSU (Fig 2) had a total of 17,878 finite elements and 12,939 nodes. To validate the T1-T2 segment for sagittal bending (flexion and extension), a pure moment of 5 Nm was applied to the superior endplate of T1 (Fig 2); the inferior nodes of T2 were fixed in all degrees of freedom (Fig 2), consistent with the referenced in-vitro study [18]. The validation efforts for the T1-T2 FSU is explained in our previous study [20]

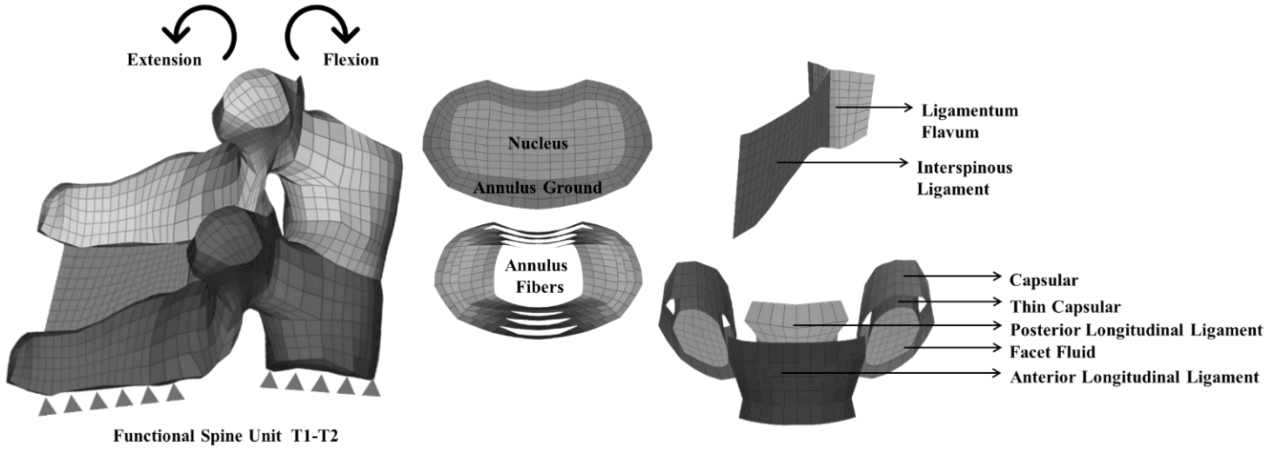

Fig.2. Represents the boundary conditions applied on the functional spine unit T1-T2 (left), the developed intervertebral disc (middle) and the ligaments of the functional spine unit (right).

The T1-T2 FSU was then integrated into the previously validated C2-T1 FEM of the cervical spine to develop the new intact C2-T2 model. The FEM consisting of the spinal column C2-T2 was given a sagittal bending with the inferior nodes of T2 were constrained and a moment load of 2Nm was applied at the superior part of C2 (Fig 3). This approach mirrored the method [19] used for the validation of the intact C2-T1 FEM, where the lowest vertebra was constrained, and a moment load was applied to the top vertebra. The ROM for each FSU in the C2-T2 model was calculated and compared against experiment corridors of C2-T1.

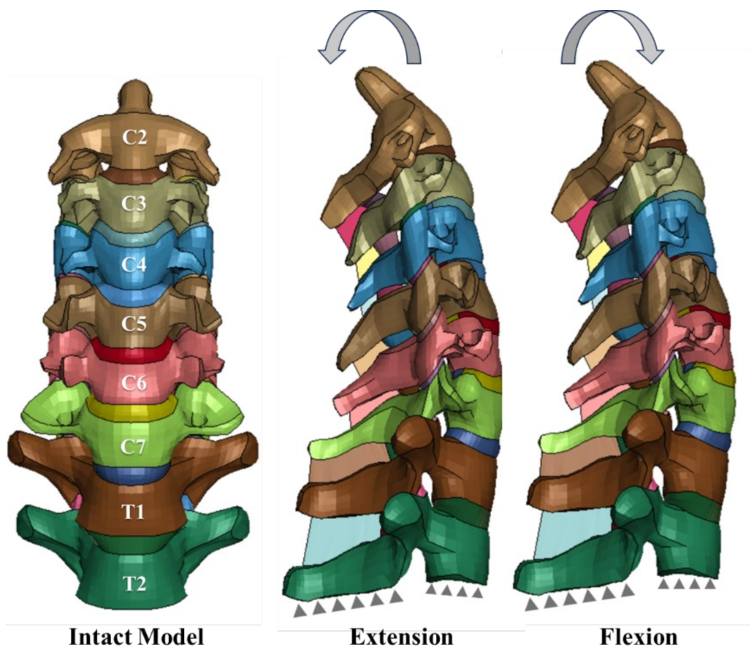

Fig.3. Represents the intact C2-T2 model (left), the boundary conditions (middle is extension and right is flexion) are shown.

III. RESULTS

The ROM at FSUs of the C2-T2 FEM was compared with the C2-T1 FEM during flexion (Fig 4) and extension (Fig 5) along the with experimental corridors [19]. During flexion, all FSUs remained within the experimental range, except for C7T1, which exceeded by 25 % when subjected to the maximum applied moment load of 2 Nm. In extension, the FSUs C34 and C56 were positioned near the upper bound of the corridor, while C45 and C7T1 fell outside the experimental limits, with the deviation being most pronounced at C7T1.

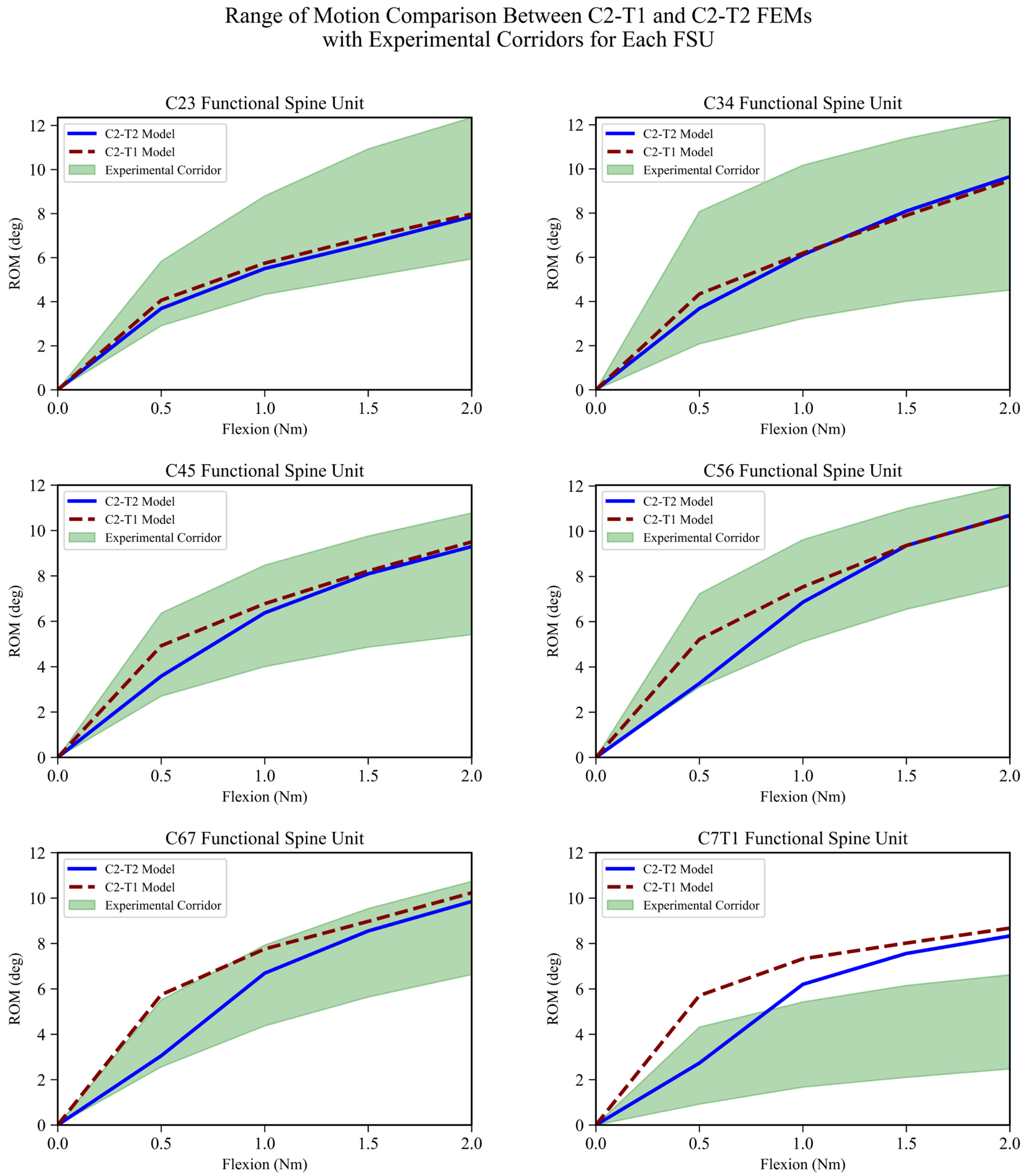

Fig.4. Represents the range of motion (ROM) at each functional spine unit (FSU) in the C2-T1 and C2-T2 FEM models during flexion with the experimental corridors [19].

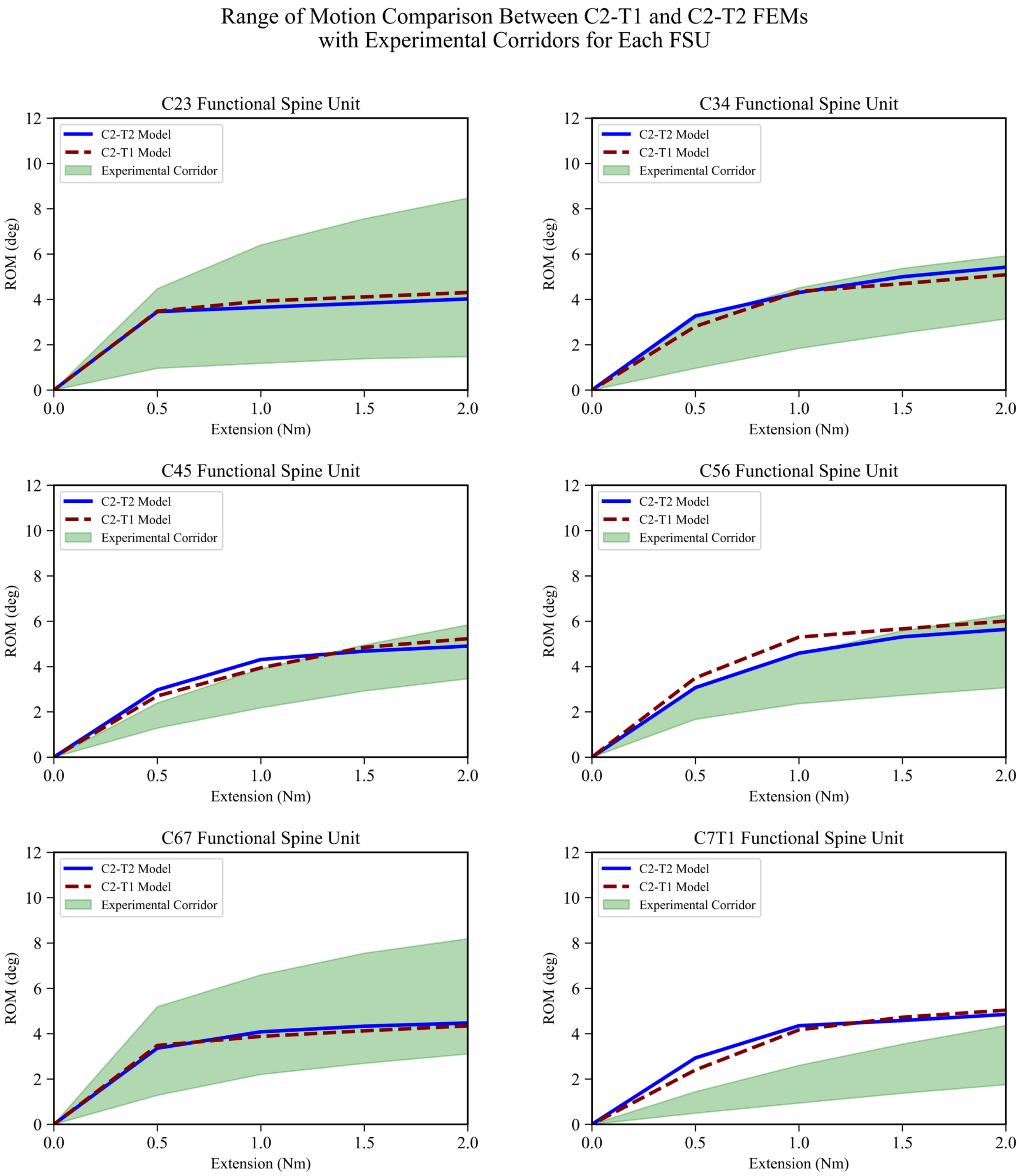

Fig.5. Represents the range of motion (ROM) at each functional spine unit (FSU) in the C2-T1 and the C2-T2 FEM models during extension with the experimental corridors [19].

The intact C2-T1 and C2-T2 models were compared (Fig. 6) to evaluate ROM variations at FSUs from C23 to C7T1 and assess the effect of incorporating the T2 vertebra in the analysis. There were minimal differences across the FSUs between the two models. During flexion, the percentage difference (Fig 7) remained within ±4%, while during extension, the variation was within ±7%. At the C2-T2 model, the ROM at FSU C7T1 was reduced by less than 4% compared to the C7T1 FSU in the C2-T1 model. Although slight variations were observed at certain FSUs, they remained within a range, suggesting that both models demonstrate similar biomechanical behaviour in sagittal plane motion.

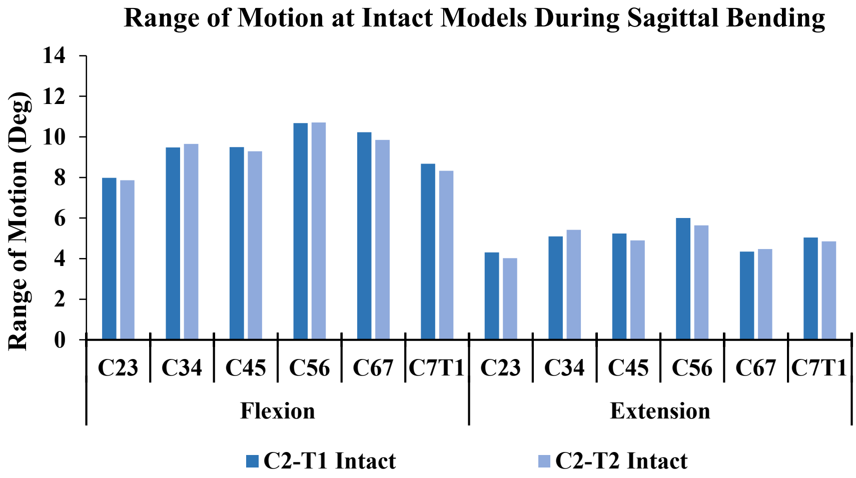

Fig.6. Shows the maximum range of motion at each functional spine unit from C23 to C71 at the C2-T1 and C2-T2 intact models.

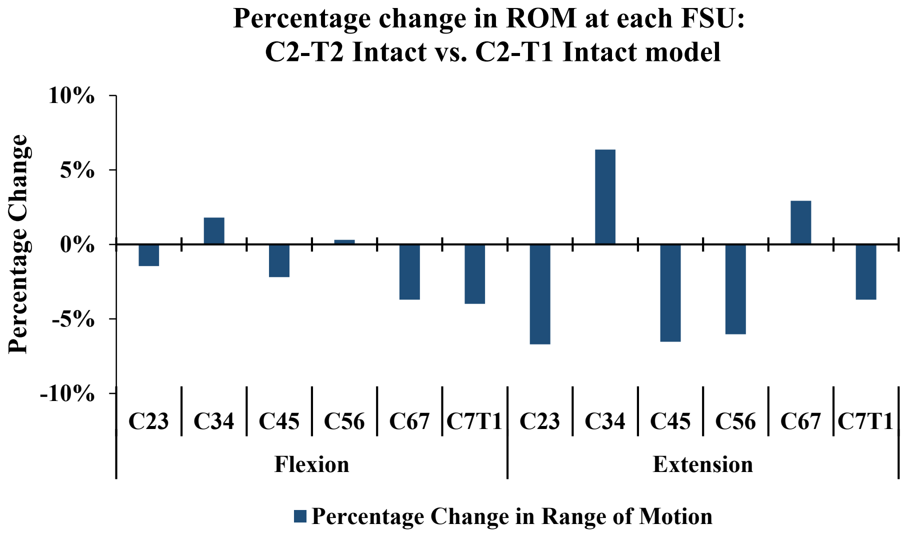

Fig.7.Shows the percentage change in range of motion at each functional spine unit at the C2-T2 intact model when compared with the C2-T1 intact model.

IV. DISCUSSION

This study evaluated whether the inclusion of the T2 vertebra in a validated C2–T1 finite element model influenced cervical spine biomechanics under sagittal bending. The T1–T2 FSU was validated earlier [20]. Comparisons between the C2–T1 and C2–T2 models for the intact case, helped assess the potential boundary condition artifacts. The ROM variations across the functional spinal units were minimal. Although the observed ROM changes were minimal, the outcomes in long fusion constructs terminating at C7 has to be studied, as kinematic changes could potentially lead to early adjacent segment degeneration or junctional failure [3-4][21]. These changes in ROM during sagittal bending can be attributed to differences in boundary conditions—applied at T1 in the experimental setup, whereas in this finite element model, they were imposed at T2, as previously discussed.

Most FEM studies employ single-loading protocols; however, the cervical spine experiences thousands of load cycles per day. The observed change in C7T1 motion also reflects the sensitivity of cervical spine models to boundary condition assumptions. It was previously demonstrated that rigidly fixing terminal vertebrae, such as T1, in PMHS models resulted in non-physiologic load paths and failure mechanisms [22]. Moreover, the kinematics show the load path changes that can be observed between the two columns. Permitting small non-zero rotations at the inferior end of cervical cantilever models can help replicate realistic boundary imperfections [23]. Additionally, accounting for vertebral geometry, material property gradients, and endplate constraints is recommended to mitigate boundary artifacts [24]. It was proposed that extending the spinal column length can also be beneficial in shifting the region of interest away from fixed boundaries [18][25].

While the C2–T1 finite element model was validated against experimental data that replicated in vitro conditions, to the authors' knowledge, no PMHS or experimental studies currently exist for a full C2–T2 spinal column. Therefore, the C2–T2 model could not be directly validated across its full extent. Nonetheless, the model was developed using anatomically accurate morphometrics and material properties, and its segmental ROM remained consistent with C2–T1 experimental corridors, with the exception of the C7T1 level, where differences may reflect the shift in boundary condition.

V. CONCLUSION

The inclusion of the T2 vertebra in the cervical spine finite element had minimal changes in the ROM, however they small variations accumulate over time especially for long fusion constructs terminating at C7. Future studies should explore various fusion surgeries, such as anterior cervical discectomy and fusion (ACDF) and posterior cervical laminectomy and fusion (PCLF), to assess the impact of the such surgical procedures at the cervicothoracic junction.

VI. ACKNOWLEDGEMENTS

Authors acknowledge the support of ANRF-SERB-CRG grant (File no CRG/2023/004727), Department of Science and Technology, India for the work. Also, acknowledge the computational support of Mr Andrews, Senior Research Fellow, SMEC and CeHMA, VIT Chennai.

VII. APPENDIX

Table 2
Represents the dimensions of the morphometric parameters used in the study as mentioned in figure 1.

Morphometric Parameter	Notation Used in Figure 1	Dimension of Parameter (mm)
Anterior Vertebral Body Height	A	17.49
Posterior Vertebral Body Height	B	20.69
Anterior-Posterior Diameter	C	16.33 (top of the vertebra) 17.86 (bottom of the vertebra)
Transverse Diameter	D	23.17 (top of the vertebra) 35.29 (bottom of the vertebra)
Pedicle Height	E	13.55 (pedicle at the left side) 13.63 (pedicle at the right side)
Pedicle Width	F	8.55 (pedicle at the left side) 9.10 (pedicle at the right side)
Spinal Canal Depth	G	17.34
Spinal Canal Width	H	19.00
Transverse Process Length	I	21.20 (transverse process at the left) 20.50 (transverse process at the right)
Spinous Process Length	J	28.35
Spinous Process Height	K	10.78

Table 3
Represents the dimensions of the other morphometric parameters used in the study as mentioned in figure 1.

Other Morphometrics Parameters	Side	Dimension of Parameter (mm)
Facet Width	Left	10.72 (top of the vertebra) 8.71 (bottom of the vertebra)
	Right	10.96 (top of the vertebra) 9.23 (bottom of the vertebra)
Facet Height	Left	14.59 (top of the vertebra) 10.51(bottom of the vertebra)
	Right	14.10 (top of the vertebra) 10.56 (bottom of the vertebra)

VIII. REFERENCES

[1] Salari, N., Darvishi, N. (2021) Global prevalence of osteoporosis among the world older adults: a comprehensive systematic review and meta-analysis. *J Orthop Surg Res*, **16**(1): p.669.

[2] Hong, C. G., Nam, W. D., Lee, Y. J., Lee, D. (2024) Effect of Osteoporosis on Clinical and Radiological Outcomes Following One-Level Anterior Cervical Discectomy and Fusion. *Asian Spine J,* **18**(2): p.182-189

[3] Harinathan, B., Jebaseelan, D., Yoganandan, N., Vedantam, A. (2024) Comparing adjacent segment biomechanics between anterior and posterior cervical fusion using patient-specific finite element modelling. *Asian Spine J* **18**(6): p.777–793.

[4] Tan, L. A., Yoganandan, N., et al. (2022) Biomechanical analysis of 3-level anterior cervical discectomy and fusion under physiologic loads using a finite element model. *Neurospine*, **19**(2): p.385–392

[5] Vedantam, A., Purushothaman, Y., et al. (2023) Spinal Cord Stress After Anterior Cervical Diskectomy and Fusion: Results from a Patient-Specific Finite Element Model. *Ann Biomed Eng,* **51**(5): p.1040-1051

[6] Panjabi, M. M., Oxland, T., et al. (1991) Thoracic human vertebrae quantitative three-dimensional anatomy. *Spine*, **16**(8): p.888–901

[7] Panjabi, M. M., Oxland, T., et al. (1993) Articular facets of the human spine: Quantitative three-dimensional anatomy. *Spine*, **18**(10): p.1298-310

[8] Ebraheim, N. A., Xu, R., Ahmad, M., & Yeasting, R. A. (1997) The quantitative anatomy of the thoracic facet and the posterior projection of its inferior facet. *Spine*, **22**(16): p.1811–1817.

[9] Singh, R., Srivastva, S. K., Prasath, C. S. V., Rohilla, R. K., Siwach, R., & Magu, N. K. (2011) Morphometric measurements of cadaveric thoracic spine in Indian population and its clinical applications. *Asian Spine J*, **5**(1): p.20–34.

[10] Kunkel, M. E., Herkommer, A., Reinehr, M., Böckers, T. M., & Wilke, H. J. (2011) Morphometric analysis of the relationships between intervertebral disc and vertebral body heights: An anatomical and radiographic study of the human thoracic spine. *J Anat*, **219**(3): p.375–387.

[11] Masharawi, Y., & Salame, K. (2011) Shape variation of the neural arch in the thoracic and lumbar spine: Characterization and relationship with the vertebral body shape. *Clin Anat*, **24**(7): p.858–867.

[12] Kaur, K., Singh, R., Prasath, V., Magu, S., Tanwar, M. (2016) Computed tomographic-based morphometric study of thoracic spine and its relevance to anaesthetic and spinal surgical procedures. *J Clin Orthop Trauma*, **7**(2): p.101–108.

[13] Choi, H., Purushothaman, Y., Ozobu, I., Yoganandan, N. (2024) Is posterior cervical foraminotomy better than fusion for warfighters?: A biomechanical study. *Mil Med*, **189**: p.710–718.

[14] John, J. D., Saravana Kumar, G., Yoganandan, N. (2019) Cervical spine morphology and ligament property variations: A finite element study of their influence on sagittal bending characteristics. *J Biomech*, **85**: p.18–26.

[15] John, J. D., Arun, M. W. J., Gurunathan, S. K., Yoganandan, N. (2017) Cervical spine finite element model with anatomically accurate asymmetric intervertebral discs. *Summer Biomechanics and Biotransport Conference*, **2017**, Tucson, AZ, USA. P.153-154

[16] Purushothaman, Y., Yoganandan, N., Jebaseelan, D., Choi, H., Baisden, J. (2020) External and internal responses of cervical disc arthroplasty and anterior cervical discectomy and fusion: A finite element modeling study. *J Mech Behav Biomed Mater*, **106**: p.103735.

[17] John, J. D., Arun, M. W., Yoganandan, N., Kumar, S. (2017) Mapping block-based morphing for subject-specific spine finite element models. *International Studies Association Conference*, **2017**, Baltimore, Maryland, USA.

[18] Liebsch, C., & Wilke, H. J. (2020) Rib presence, anterior rib cage integrity, and segmental length affect the stability of the human thoracic spine: An in vitro study. *Front Bioeng Biotechnol*, **8**: 46.

[19] Wheeldon, J. A., Pintar, F. A., Knowles, S., Yoganandan, N. (2006) Experimental flexion/extension data corridors for validation of finite element models of the young, normal cervical spine. *J Biomech*, **39**(2): p.375–380.

[20] Asir J. A., Kalaimani, P.S., et al. (2024) Finite element modelling and validation of T1-T2 functional spine unit: A developmental study. *TRAFFIC INJURY PREVENTION*, **25**: p.S224-S226.

[21] Kumaresan, S., Yoganandan, N., & Pintar, F. A. (1999) Finite element analysis of the cervical spine: A material property sensitivity study. *Clin Biomech (Bristol)*, **14**(1): p.41-53.

[22] Nightingale, R. W., Doherty, B. J., et al. (1991) Influence of end condition on human cervical spine injury mechanisms. *Proceedings - Society of Automotive Engineers, p.391-399.*

[23] Noone, G., Ang, W. T. (1996) The inferior boundary condition of a continuous cantilever beam model of the human spine. *Australas Phys Eng Sci Med,* **19**(1): p.26-30

[24] Belytschko, T., Schwer, L., Privitzer, E. (1978) Theory and application of a three-dimensional model of the human spine. *Aviat Space Environ Med,* **49**(1): p.158-165

[25] Kettler, A., Wilke, H.-J., Haid, C., Claes, L. (2000) Effects of Specimen Length on the Monosegmental Motion Behavior of the Lumbar Spine. *Spine*, **25**(5): p.543-550